Food and Chemical Toxicology 134 (2019) 110867

Contents lists available at ScienceDirect

Food and Chemical Toxicology

journal homepage: www.elsevier.com/locate/foodchemtox

# Exploration of the binding between ellagic acid, a potentially risky food additive, and bovine serum albumin

Fengru Liu[1], Yiyin Zhang[1], Qiuyang Yu, Yizhong Shen*, Zhi Zheng, Jieshun Cheng, Wencheng Zhang, Yingwang Ye**

*Engineering Research Center of Bio-Process, Ministry of Education, School of Food & Biological Engineering, Hefei University of Technology, Hefei, 230009, China*

ARTICLE INFO

*Keywords:*
Ellagic acid
Bovine serum albumin
Combination mechanism
Toxicity
Molecular docking

ABSTRACT

Ellagic acid (EA), a natural plant polyphenol, is usually used as a functional additive in variety of health foods. However, the potential toxicity of EA to human health should be paid enough attention. To clarify its biological toxicity *in vivo*, this study explored the binding mechanism of EA with bovine serum albumin (BSA) by means of spectroscopic approaches and molecular docking insimulative physiological conditions. The results showed that the mixture of BSA with EA could spontaneously cause the formation of BSA-EA complex through electrostatic interaction under simulative physiological conditions (0.01 mol·L$^{-1}$Tris-HCl, 0.015 mol L$^{-1}$ NaCl, pH = 7.4). Molecular docking experiments revealed that EA was primarily bound to the hydrophobic pocket of the site I (subdomain IIA) of BSA. It has been reported that the binding of small functional molecules to serum albumins remarkably impacts their absorption, distribution, metabolism, and excretion features. Therefore, this study might be helpful for human to have an in-depth understanding of the biological effect of EA *in vivo* and guide human to take it safely and reasonably.

## 1. Introduction

Ellagic acid ($C_{14}H_6O_8$, EA), a dimeric derivative of gallic acid, is a natural polyphenolic component widely found in pomegranate, strawberry, longan seed, mango kernel, walnut, tea and other plant tissues (Huerga-Gonzalez et al., 2015; Soong and Barlow, 2006; Yang and Tomas-Barberan, 2019). Recently, people have begun to pay attention to its role in the management of various oxidative stress-related diseases, including metabolic syndrome, cardiovascular dysfunction and cancer (Larrosa et al., 2010). A large number of studies have shown that EA has a series of beneficial effects on human body, such as antioxidant (Ma et al., 2018), antiviral (Promsong et al., 2018), anticancer (Zhong et al., 2019), anti-bacterial (Beshbishy et al., 2019), anti-inflammatory (El-Shitany et al., 2014), inhibition of diabetic nephropathy (Zhou et al., 2019), inhibition of obesity (Wang et al., 2013b). Due to its excellent health effects, it is becoming more and more popular and widely used in the field of food and medicine. It is worth noting that, due to its toxic effects, the long-term consumption of EA may cause congestion in some organs and endanger human health (Tasaki et al., 2008). Considering its toxicity and food safety, the dosage of EA as health food additive should be controlled within a safe range. In addition, the long-term use of EA can lead to accumulation in the body, and the potential toxic residues in the excreta may pose a potential risk to environmental safety.

Serum albumin is the most abundant protein in various biological circulatory systems and plays a leading role in drug distribution, efficacy and toxicity. Many drugs and other bioactive molecules reversibly bind to serum albumin, which significantly affects the absorption, distribution, metabolism and excretion of drugs and bioactive compounds (Schmidt et al., 2010; Xu et al., 2012; Yang et al., 2014). Exploring the molecular interaction mechanism between bioactive molecule and protein during the transport process is a necessary condition for determining the release efficiency of active molecule from the carrier and predicting the effectiveness of active molecule. Certain amino acids in the bovine serum albumin (BSA) molecule have the property of absorbing ultraviolet light and emitting fluorescence, and are often used as model proteins for the determination of reactivity with phenolic substances (Papadopoulou et al., 2005). The binding constants, binding distance, energy transfer, mechanism of action (electrostatic interaction, hydrogen bond, van der Waals force, etc.) and action sites through

* Corresponding author.
** Corresponding author.
*E-mail addresses:* yzshen@hfut.edu.cn (Y. Shen), yeyw04@mails.gucas.ac.cn (Y. Ye).
[1] These authors contributed equally to this work.

https://doi.org/10.1016/j.fct.2019.110867
Received 27 August 2019; Received in revised form 17 September 2019; Accepted 1 October 2019
Available online 03 October 2019

computer simulation have been reported in many literatures (Garzon et al., 2015; Ishtikhar et al., 2018; Khatun et al., 2018). At present, the research on EA mainly focuses on purification, separation and content determination (Chen et al., 2019; Huerga-Gonzalez et al., 2015; Szmagara et al., 2019). Although EA has a wide range of pharmacological effects, its effects on plasma protein and its mechanism of action need to be further studied (Nanda et al., 2007), especially the toxicity and the safety evaluation of EA to human health is rarely reported from the molecular structure of EA.

The interaction between EA and BSA was studied by using spectroscopy techniques (including fluorescence spectroscopy and UV–vis spectroscopy) and molecular simulation techniques. The Stern-Volmer equation is used to determine the type of annihilation, and the static quenching formula is used to obtain the binding constant K and the number of binding sites n. The type of action between EA and BSA was determined by Van't Hoff equation, and the mode of action between EA and BSA was discussed. Furthermore, the Surflex-Dock program was used to study the molecular docking between EA and BSA. The results of spectral experiments and molecular docking theory were compared to study the interaction between EA and BSA from both experimental and theoretical aspects. The results are helpful to understand the transport and distribution of EA with pharmacological activity *in vivo*, and lay a theoretical foundation for the study on the mechanism, kinetics and toxicology of EA *in vivo*.

## 2. Materials and methods

### 2.1. Reagents and apparatus

All chemicals and biological reagents were obtained from commercial suppliers and used without further purification. EA (98% purity) was purchased from Aladdin Reagent Co. (Shanghai, China). BSA (purity>98%) was purchased from Sigma-Aldrich Chemical Corporation (St Louis, MO, USA). Tris-HCl buffer solutions with different pH were prepared. The water used throughout was ultrapure water.

A Hitachi F-4500 spectrofluoro photometer (Hitachi Company, Tokyo, Japan) equipped with a thermostat bath and 1.0 cm quartz cell was used to record all fluorescence data. A UV-2450 spectrophotometer (Tianmei Corporation, Shanghai, China) equipped with 1.0 cm quartz cell was applied to adopt UV–vis absorption spectra. A PHS-3C pH meter (Leici, Shanghai, China) was used to adjust the pH values of the aqueous solutions.

### 2.2. Sample preparation

BSA ($1.0 \times 10^{-5}$ mol $L^{-1}$) and EA ($1.0 \times 10^{-5}$ mol $L^{-1}$) solution were prepared with 0.01 mol $L^{-1}$ Tris-HCl (0.015 mol $L^{-1}$ NaCl) at pH = 7.4. The buffer was filtered through a 0.45 μm syringe filter. Double-distilled water was used for all the experiments. EA stock solutions were prepared in ethanol (> 99%) and then diluted with Tris-HCI to obtain the desired concentrations. All reserve solutions should be stored in dark at 4 °C. All chemicals were of analytical grade and used without further purification.

### 2.3. Measurement of ultraviolet–visible absorption spectrum

The ultraviolet–visible absorption measurements were recorded using a UV–vis 1010 Spectrometer at a scan rate of 10 nm/s with 1.0 cm-path-lengthquartz cuvette in the visible wavelength range of 200–450 nm at 298 K (Rudradip et al., 2017). Absorption spectra were obtained with fixed concentrations of BSA and EA ($1.0 \times 10^{-5}$ mol $L^{-1}$).

### 2.4. Measurement of steady state fluorescence spectrum

The fluorescence spectrum of BSA in the absence and presence of EA was measured using an F-4500 fluorescence spectrophotometer equipped with a 1.0 cm quartz cell. The concentration of BSA is fixed at $1.0 \times 10^{-5}$ mol $L^{-1}$, and the concentration of EA is changed from 0.0 to $1.8 \times 10^{-5}$ mol $L^{-1}$, and the increment of each step is $0.2 \times 10^{-5}$ mol $L^{-1}$. Samples were placed in Tris-HCI for 60 min at 283 K, 300 K and 310 K prior to fluorescence measurement. Fluorescence emission spectra with an excitation wavelength of 280 nm and a scanning wavelength range of 300 nm–450 nm were recorded. The excitation and emission slit widths are both 5 nm (Rudradip et al., 2017).

### 2.5. Molecular docking

This experiment simulates molecular docking using the Surflex-Dock program in SYBYL-X 2.1.1 for protein structure of BSA (PDB ID: 3V03) available from PDB (http://www.pdb.org). Protein preparation was performed using SYBYL-X's protein preparation tool. Remove all water molecules and add hydrogen atoms. The energy is then minimized using a distance dependent dielectric Tripos Force Field. Finally, the BSA molecule was charged using the AMBER7F9902 method. The 2D structure of ellagic acid was converted to a 3D structure using the Concord 3D program in SYBYL-X 2.1.1, followed by energy optimization using Tripos Force Field.

## 3. Results and discussion

### 3.1. UV–visible spectroscopy analysis of EA-BSA system

The absorbed wavelength and absorption efficiency will change with the structure and the environment of the molecules, therefore UV–vis absorption spectroscopy technique can be used to investigate the structural changes and complex formation between proteins and ligands (He et al., 2014; Makarska-Bialokoz and Lipke, 2019). The absorption spectrum of BSA without or with EA was shown in Fig. 1. Curve a (BSA only) displayed two absorption peaks. The strongabsorption peak around 210 nm not only reflects the framework conformation of protein but also corresponds to the peptide bond. The weak absorption peak around 280 nm appears due to the presence of aromatic amino acids (Trp, Tyr and Phe) in BSA molecule (He et al., 2014). According to thecurve b, it can be discovered that the two peaks in the ultraviolet region of BSA shifted to the direction of long wavelength and the absorbance intensity increased with addition of EA, which implies the existence of bathochromic effect. The enhanced

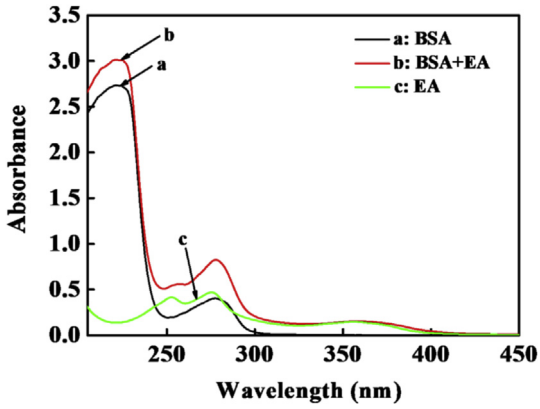


**Fig. 1.** UV–Visible absorption spectra of BSA in the absence and presence of EA in 0.01 mol·$L^{-1}$Tris-HCl (0.015 mol $L^{-1}$ NaCl) at pH = 7.4. (a) The absorption spectrum of BSA only; (b) the absorption spectrum of BSA-EA complex; (c) the absorption spectrum of EA only. c (BSA) = c (EA) = $1.0 \times 10^{-5}$ mol $L^{-1}$.

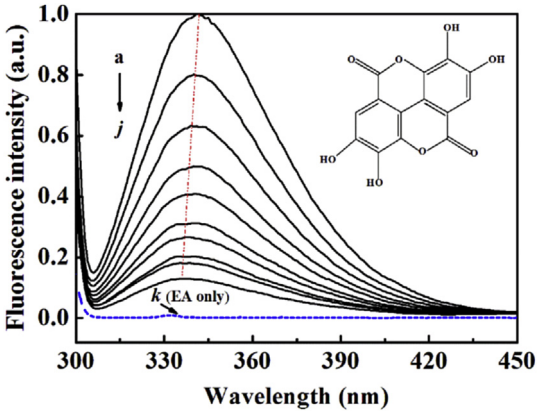


**Fig. 2.** Fluorescence emission spectra of BSA in the absence and presence of EA in 0.01 mol·L$^{-1}$Tris-HCl (0.015 mol L$^{-1}$ NaCl) at pH = 7.4. c (BSA) = 1.0 × 10$^{-5}$ mol L$^{-1}$; c (EA)/(10$^{-5}$ mol L$^{-1}$), a–j: from 0.0 to 1.8 at increments of 0.2; curve *k* (dashed line) shows the emission spectrum of EA only (T = 298 K, λex = 295 nm). The insert corresponds to the molecular structure of EA.

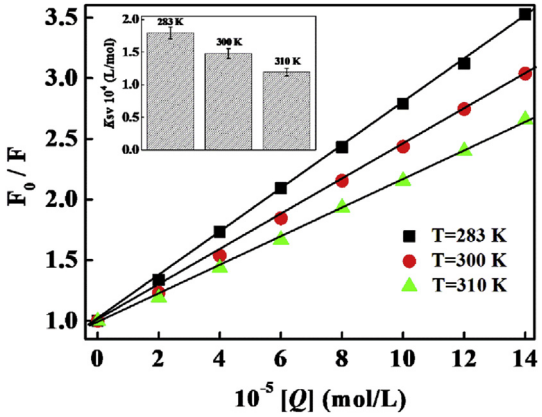


**Fig. 3.** Stern-Volmer plots for the quenching of BSA by EA at different temperatures in 0.01 mol L$^{-1}$ Tris-HCl (0.015 mol L$^{-1}$ NaCl) at pH = 7.4. (BSA, 1.0 × 10$^{-5}$ mol L$^{-1}$). The inset shows the relationship between the Stern-Volmer quenching constants *K*sv and temperature *T*.

absorption peak at 280 nm is caused by the π-π* transition of aromatic heterocycle (Trp and Tyr) in the BSA molecule (Patil et al., 2007). The enhanced absorption peak of 210 nm was mainly caused by the *n*-π* transition of the C═O group on the peptide bond. The interaction between EA and BSA in solution causes the peptide chain to stretch, which induces the exposure of aromatic heterocyclic hydrophobic groups surrounded in the molecule of BSA, and finally leads to the enhancement of absorption peak at 280 nm (Chi et al., 2010; Makarska-Bialokoz and Lipke, 2019). The result implied that the EA-BSA complex was formed.

### 3.2. Fluorescence characteristics of EA-BSA system

Fluorescence quenching is a sensitive and effective method for studying the interaction of small molecules with proteins. The fluorescence spectra of BSA in the absence and presence of different EA concentrations were measured in the concentration range of 300–450 nm upon excitation at 280 nm. There was no native fluorescence emission for EA at the range measured and it caused linear quenching of the BSA fluorescence intensity (Fig. 2) with a slight red shift of the emission maximum, which may arise from the increase polarity of the EA-BSA system. The results also indicate the formation of a non-fluorescent complex upon the interaction of EA and BSA.

Due to the presence of Trp and Tyr residues, BSA can produce intrinsic fluorescence (Quiming et al., 2005). BSA exhibits a maximum peak characteristic fluorescence emission spectrum at 340 nm when excited at 280 nm. The binding of EA to BSA was monitored by measuring changes in the intrinsic fluorescence phenomenon of BSA (fluorophore) in the presence and absence of EA (quencher). Fig. 2 shows that when a gradual increase in the amount of EA is added to a fixed concentration of BSA under simulated physiological conditions (pH = 7.4, 310 K), the maximum emission peak of BSA decreases regularly. Fluorescence quenching occurs due to the molecular interaction of the fluorophore with the quencher. As shown in Fig. 2, the significant quenching of BSA fluorescence intensity after the addition of EA indicates the binding of EA to BSA. In ligand-protein binding studies, we have utilized the Scatchard equation for calculation of binding constant and number of binding sites (Eq. (3)). A linearity relationship was seen between r/D$_f$ and r (Where, r is the number of moles of EA bound to 1 mol of BSA, D$_f$ is the concentrations of free EA).

Fluorescence quenching can be classified into static and dynamic quenching, which can be distinguished by their different dependence on temperature. The static quenching is caused by the ground state complex formed by fluorophore and quenching agent, and the dynamic quenching is caused by the molecular collision between ligand and fluorophore. For dynamic quenching, the quenching constant increases with the increase of temperature, while the quenching constant of static quenching decreases with the increase of temperature (Zhang et al., 2012). The possible quenching mechanism can be explained by Stern-Volmer equation.

Stern-Volmer equation (Eq. (1)) (Bose, 2016) was used to analyze the fluorescence data and determine $K_{SV}$ by thelinear regression of a plot $F_0/F$ against [$Q$].

$$\frac{F_0}{F} = 1 + K_{SV}[Q] = 1 + K_q\tau_0[Q] \quad (1)$$

where $F_0$ and $F$ are the fluorescence intensities without and with ligand molecule respectively, $K$q is the bimolecular quenching constant, $\tau_0$ is the lifetime of the fluorophore in the absence of the quencher, [$Q$] is the concentration of the quencher, and $K_{SV}$ is the Stern-Volmer quenching constant.

Fig. 3 shows the stern-volmer quenching of ellagic acid in the presence of BSA at different temperatures (283, 300 and 310 K), which demonstrates a linear relationship. A linear Stern-Volmer plot is generally indicative of a single class of fluorophores in a protein, all equally accessible to the quencher; this also means that only one mechanism (dynamic or static) of quenching occurs (Li and Wang, 2015). $K_{SV}$ value is determined by the slope of $F_0/F$ and [$Q$] curve, and corresponding $K_{SV}$ value is listed in Table 1. The results showed that $K_{SV}$ value decreased with the increase of temperature, which indicated that the possible quenching mechanism of BSA fluorescence through EA interaction was static quenching. In addition, it should be noted that the dynamic quenching process only affects the excited states of the fluorophores without modifying their UV–vis absorption spectrum. However, static quenching usually causes changes in the UV–vis absorption spectrum (Makarska-Bialokoz and Lipke, 2019). UV–vis absorption experiments can further confirm the results of fluorescence studies (Fig. 2).

**Table 1**
Stern-Volmer quenching constants for the interaction of BSA with EA at various temperatures.

| pH | *T* (K) | 10$^4$*K*sv (L·mol$^{-1}$) | *R*[a] | *S.D.*[b] |
|---|---|---|---|---|
| 7.4 | 283 | 1.7933 | 0.9998 | 0.01956 |
| | 300 | 1.4780 | 0.9997 | 0.02057 |
| | 310 | 1.1943 | 0.9996 | 0.01830 |

[a] *R* is the correlation coefficient*K*sv values.
[b] *S.D.* is the standard deviation for the *K*sv values.

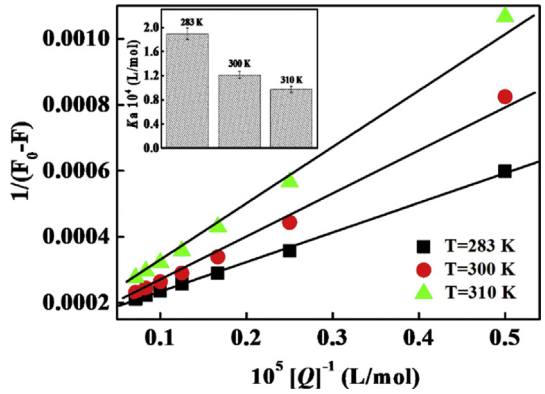


**Fig. 4.** Lineweaver-Burk curves for the BSA-EA system at three different temperatures in 0.01 mol·L$^{-1}$Tris-HCl (0.015 mol L$^{-1}$ NaCl) at pH = 7.4. (BSA, $1.0 \times 10^{-5}$ mol L$^{-1}$). The inset shows the relationship between the binding constant *Ka* and temperature *T*.

Fig. 4 is the Lineweaver-Burk quenching diagram of BSA-EA at three temperatures, which can be obtained from the lineweaver-Burk equation (Eq. (2)) (Abdelhameed et al., 2017):

$$\frac{1}{F_0 - F} = \frac{1}{F_0} + \frac{1}{K_a F_0} \times \frac{1}{[Q]} \quad (2)$$

It also shows a linear relationship. The results showed that the static quenching induced by EA-BSA complex played a leading role in the fluorescence quenching process, but not the dynamic collision quenching.

### 3.3. Binding constant and number of binding sites of EA-BSA system

The equilibrium fraction of bioactive compound is an important pharmacokinetic parameter, which influences bioactive compound elimination and distribution in the body. For a binding equilibrium system, the binding constant of EA-BSA complex can be calculated according to the Scatchard model. The Scatchard plot is defined by equation (Eq. (3)) (Li and Wang, 2015).

$$r/D_f = nK_b - rK_b \quad (3)$$

where *r* represents the number of moles of bound EA per mole of BSA, n represents the number of binding sites on the BSA molecule, $K_b$ is the binding constant, [$D_f$] is the concentration of EA.

The Scatchard plot for EA-BSA complex which relates the value of *r*/[$D_f$] to the value of *r* is presented in Fig. 5. The Scatchard plot is a straight line, which means that the EA binds independently to a set of equivalent sites on BSA and supports the use of the independent binding

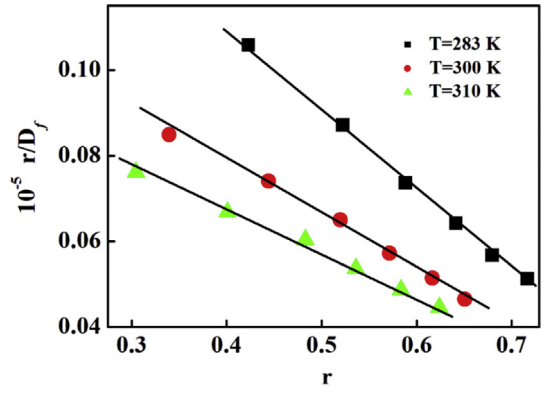


**Fig. 5.** Scatchard curves for the BSA-EA system at three different temperatures in 0.01 mol·L$^{-1}$Tris-HCl (0.015 mol L$^{-1}$ NaCl) at pH = 7.4. (BSA, $1.0 \times 10^{-5}$ mol L$^{-1}$).

site model. The results showed that EA-BSA at different temperatures in plasma could be stored and transported from the circulatory system to the target site to achieve biological activity.

The number of binding sites was calculated according to the following equation (Eq. (4)) (Wang et al., 2009):

$$\log\frac{F_0 - F}{F} = \log Ka + n\log[Q] \quad (4)$$

where $K_a$ denotes the binding constant, n is a number of binding sites, and [*Q*] represents the final concentration of quencher. The number of binding sites of EA-BSA at three temperatures of 283, 300 and 310 K were calculated, as shown in Table 2, which were 0.98, 1.03 and 1.07 respectively. The three data are approximately 1, indicating that one BSA molecule can bind to one ellagic acid molecule (Ali and Al-Lohedan, 2017). The results are similar to those of other bioactive compounds interacting with BSA molecules (Krishnan et al., 2018; Makarska-Bialokoz and Lipke, 2019; Trnkova et al., 2011). At the same time, the three constants of $K_{SV}$, $K_a$ and $K_b$ are all on the order of $10^{-4}$, indicating that the binding force of EA and BSA is strong.

### 3.4. Thermodynamic parameters and binding characteristics of EA-BSA system

Interactions between small molecules and large biological molecules are mainly based on various weak non-covalent reaction forces, such as hydrophobic forces, electrostatic interactions, van der Waals interactions, hydrogen bonds, etc (Wang et al., 2013a). The binding model of EA to BSA can be determined from the calculation of thermodynamic parameters, including enthalpy changes ($\Delta H$), entropy changes ($\Delta S$) and Gibbs free energy changes ($\Delta G$). Meanwhile, the thermodynamic parameters of the combined process can be determined by Van't Hoff equation and thermodynamic formula (Tang and Jia, 2013).

$$\ln Ka = -\frac{\Delta H}{RT} + \frac{\Delta S}{R} \quad (5)$$

$$\Delta G = \Delta H - T\Delta S \quad (6)$$

where *R* is the gas constant (8.314 J K$^{-1}$ mol$^{-1}$), *T* is the experimental temperature and *Ka* is the binding constant at corresponding *T*.

Fig. 6 shows the corresponding plot of ln*K*a vs. $T^{-1}$. $\Delta H$ and $\Delta S$ are obtained by the slope and intercept of the linear curve, where $\Delta H$ does not significantly vary over the studied temperature range. $\Delta H$, $\Delta S$ and $\Delta G$ values at three temperatures obtained from Eqs. (5) and (6) are collected in Table 2. The negative sign for $\Delta G$ means that the interaction process is spontaneous. It is generally believed that, when $\Delta H > 0$ and $\Delta S < 0$, the interaction between the two molecules is mainly electrostatic attraction and hydrophobic interaction; when $\Delta H < 0$, $\Delta S < 0$, is mainly hydrogen bond and van der Waals force; when $\Delta H > 0$, $\Delta S > 0$, the hydrophobic force is the main force; when $\Delta H < 0$, $\Delta S > 0$, the electrostatic attraction plays a major role in the binding (Chen et al., 2018; Hazra et al., 2013). As shown in Table 2, $\Delta G$ is negative, indicating that the combination between EA and BSA is spontaneous. The negative $\Delta H$ and positive $\Delta S$ indicate that electrostatic attraction may play a major role in the binding between EA and BSA (Zhang et al., 2009).

### 3.5. Binding distance between EA and BSA

According to Föster's non-radiative energy transfer theory (Cui et al., 2004), the energy transfer will happen under conditions: (i) the donor can produce fluorescence light; (ii) fluorescence emission spectrum of the donor and UV absorbance spectrum of the acceptor have more overlap; (iii) the distance between the donor and the acceptor is approach and lower than 7 nm. The energy transfer effect is related not only to the distance between the acceptor and the donor, but also to the critical energy transfer distance. The binding distance between EA and

**Table 2**
Binding constants and relative thermodynamic parameters of BSA-EA system in 0.01 mol·L$^{-1}$Tris-HCl (0.015 mol L$^{-1}$ NaCl) at pH = 7.4.

| T (K) | Lineweaver-Burk Method | | Scatchard Method | | $\Delta H$ (KJ·mol$^{-1}$) | $\Delta S$ (J·mol$^{-1}$·K$^{-1}$) | $\Delta G$ (KJ·mol$^{-1}$) |
|---|---|---|---|---|---|---|---|
| | $10^4 Ka$ (L·mol$^{-1}$) | $R^a$ | $10^4 K_b$(L·mol$^{-1}$) | n | | | |
| 283 | 1.8949 | 0.9980 | 1.8842 | 0.98 | | | −23.17 |
| 300 | 1.2150 | 0.9991 | 1.2453 | 1.03 | −18.02 | 18.21 | −23.48 |
| 310 | 0.9749 | 0.9999 | 0.9898 | 1.07 | | | −23.67 |

[a] $R$ is the correlation coefficient for $Ka$ values.

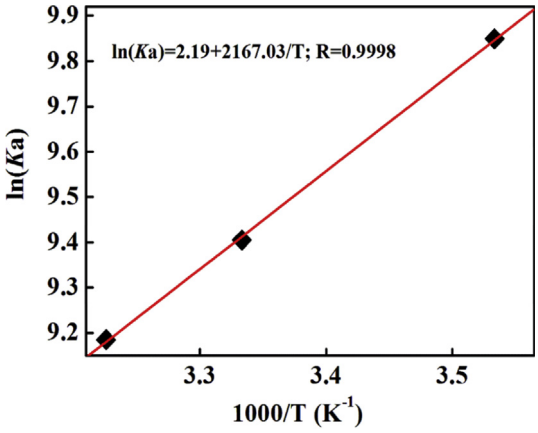


**Fig. 6.** Van't Hoff plot of BSA-EA system in 0.01 mol·L$^{-1}$Tris-HCl (0.015 mol L$^{-1}$ NaCl) at pH = 7.4.

BSA can be calculated by the equation of energy transfer efficiency (E, Eq. (7)) (Chen et al., 2011).

$$E = 1 - \frac{F}{F_0} = \frac{R_0^6}{R_0^6 + r^6} \tag{7}$$

where E denotes the efficiency of transfer between the donor and the acceptor, r is the average distances between donor and acceptor, and $R_0$ is the critical distance when the efficiency of transfer is 50%, which can be calculated by the following equation:

$$R_0^6 = 8.79 \times 10^{-25} K^2 n^{-4} \varphi J \tag{8}$$

In Eq. (8), $K^2$is the orientation factor related to the geometry of the donor and acceptor of dipoles and $K^2 = 2/3$ for random orientation in fluid solutions, n is the average refractive index of the medium in the wavelength range where spectral overlap is significant, Ø is the fluorescence quantum yield of the donor, and J is the effect of spectral overlap between the emission spectrum of the donor and the absorption spectrum of the acceptor (Fig. 7), which can be calculated by the

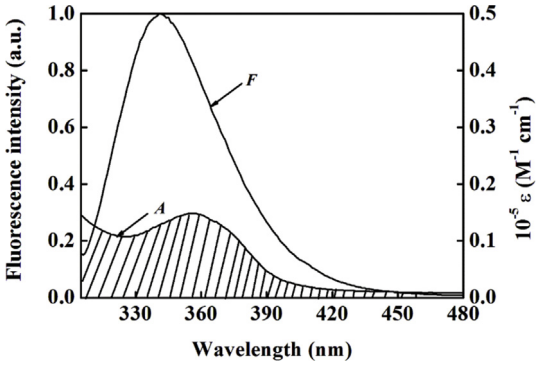


**Fig. 7.** Spectral overlap of EA absorption (*A*) with BSA fluorescence (*F*) in0.01 mol·L$^{-1}$Tris-HCl (0.015 mol L$^{-1}$ NaCl) at pH = 7.4. c (BSA) = c (EA) = $1.0 \times 10^{-5}$ mol L$^{-1}$.

equation:

$$J = \frac{\int_0^\infty F(\lambda)\varepsilon(\lambda)\lambda^4 d\lambda}{\int_0^\infty F(\lambda) d\lambda} \tag{9}$$

where F(λ) is the corrected fluorescence intensity of the donor in the wavelength range, from λ to λ+Δ λ (305–460 nm), and $\varepsilon(\lambda)$ is the extinction coefficient of the acceptor at wavelength λ.

In the present case, n = 1.36, ϕ = 0.15, and according to Eqs. (7)–(9), we calculate $J = 1.42 \times 10^{-14}$ cm$^3$ L·mol$^{-1}$, E = 0.68, $R_0$ = 2.67 nm and the binding distance is r = 2.35 nm. The values for $R_0$ and r are on the 2–8 nm scale, and $0.5R_0 < r < 1.5R_0$, which indicated a fair possibility of energy transfer from BSA to EA. It accord with conditions of Föster's non-radiative energy transfer theory, indicating again the static quenching interaction between EA and BSA (Cui et al., 2004).

### 3.6. Molecular modelling and docking of EA to BSA

Through molecular docking, we can better understand the docking morphology of secondary structure of protein, and intuitively analyze the binding site and interaction type of drug and BSA (Chen et al., 2018; Das et al., 2018; Khatun et al., 2018). Fig. 8 shows that ellagic acid has been successfully docked into the BSA, and it binds to the siteI (subdomain IIA) of structuraldomainof BSA. EA is linked and bound to BSA by four amino acid residues, Tyr160, Tyr137, Leu115 and His145. The interaction of ellagic acid with two Tyr residues further demonstrates that EA can quench the endogenous fluorescence of BSA.

## 4. Conclusions

The binding interactions in the system BSA-EA have been investigated. The obtained results showed the significant quenching of the BSA intrinsic fluorescence by EA through the mechanism of static quenching, as a consequence of complexes formation between BSA and EA. The values of all the determined parameters ($K_a$, $K_{SV}$, $K_b$, r, $R_0$, $\Delta H$, $\Delta S$ and $\Delta G$ values) confirmed the existence of static quenching. As it was stated before, in the experiments studied, the electrostatic interactions were presumably the major forces in formation of the associated complexes. EA binds to BSA at site I with a binding site number of about 1. The EA-BSA complex is mainly bonded by hydrogen bonds of residues including Tyr160, Tyr137, Leu115 and His145. The results obtained herein have benefits for revealing the binding mechanism of EA with serum albumin. Meanwhile, it might provide a fundamental insight on the relationship of the structures of EA with their absorption and biological toxicity effects *in vivo*.

## Declaration of competing interest

The authors declare that they have no known competing financial interests or personal relationships that could have appeared to influence the work reported in this paper.

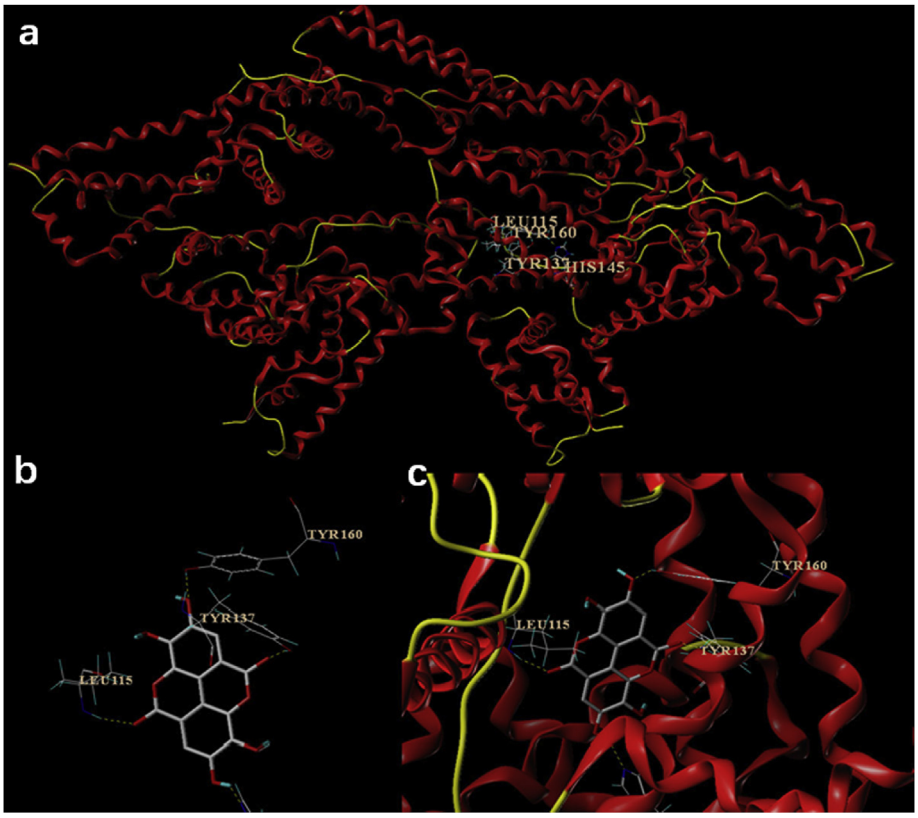


**Fig. 8.** (a) Main interaction of EA binding to the BSA at site I. (b) Hydrogen bond formed between EA and amino acids of BSA. (c) Molecular contacts between EA and amino acids of BSA.

## Acknowledgements

This work was supported by the National Key Research and Development Program (2017YFC1601202), the National Natural Science Foundation of China (21804029, 31701638, 31671951), the Natural Science Foundation of Anhui Province, China (1908085QB67),the China Postdoctoral Science Foundation (2018M632525, 2019M651770), and the Fundamental Research Funds for the Central Universities of China (Grant No. PA2019GDPK0084).

## References

Abdelhameed, A.S., Alanazi, A.M., Kadi, A.A., 2015. Spectrofluorimetric study of finasteride and bovine serum albumin interaction and its application for quantitative determination of finasteride in tablet dosage form. Anal. Methods 7, 5096–5102.

Ali, M.S., Al-Lohedan, H.A., 2017. Deciphering the interaction of procaine with bovine serum albumin and elucidation of binding site: a multi spectroscopic and molecular docking study. J. Mol. Liq. 236, 232–240.

Beshbishy, A.M., Batiha, G.E.S., Yokoyama, N., Igarashi, I., 2019. Ellagic acid microspheres restrict the growth of babesia and theileria in vitro and babesia microti *in vivo*. Parasites Vectors 12, 269.

Bose, A., 2016. Interaction of tea polyphenols with serum albumins: a fluorescence spectroscopic analysis. J. Lumin. 169, 220–226.

Chen, R., Li, J.X., Yang, Z.W., Gao, F., Qi, P.Y., Li, X., Zhu, F.M., Li, J., Zhang, J.J., 2019. Determination of ellagic acid in wine by solid-phase extraction-ultra-high performance liquid chromatography-tandem mass spectrometry. Food Anal. Method 12, 1103–1110.

Chen, T.T., Zhu, S.J., Cao, H., Shang, Y.F., Wang, M.A., Jiang, G.Q., Shi, Y.J., Lu, T.H., 2011. Studies on the interaction of salvianolic acid B with human hemoglobin by multi-spectroscopic techniques. Spectrochim. Acta 78, 1295–1301.

Chen, Y.S., Zhou, Y.F., Chen, M., Xie, B.J., Yang, J.F., Chen, J.G., Sun, Z.D., 2018. Isorenieratene interaction with human serum albumin: multi-spectroscopic analyses and docking simulation. Food Chem. 258, 393–399.

Chi, Z.X., Liu, R.T., Teng, Y., Fang, X.Y., Gao, C.Z., 2010. Binding of oxytetracycline to bovine serum albumin: spectroscopic and molecular modeling investigations. J. Agric. Food Chem. 58, 10262–10269.

Cui, F.L., Fan, J., Li, J.P., Hu, Z.D., 2004. Interactions between 1-benzoyl-4-p-chlorophenyl thiosemicarbazide and serum albumin: investigation by fluorescence spectroscopy. Bioorg. Med. Chem. 12, 151–157.

Das, S., Karn, A., Sarmah, R., Rohman, M.A., Koley, S., Ghosh, P., Roy, A.S., 2018. Characterization of non-covalent binding of 6-hydroxyflavone and 5,7-dihydroxyflavone with bovine hemoglobin: multi-spectroscopic and molecular docking analyses. J. Photochem. Photobiol., B 178, 40–52.

El-Shitany, N.A., El-Bastawissy, E.A., El-desoky, K., 2014. Ellagic acid protects against carrageenan-induced acute inflammation through inhibition of nuclear factor kappa B, inducible cyclooxygenase and proinflammatory cytokines and enhancement of interleukin-10 via an antioxidant mechanism. Int. Immunopharmacol. 19, 290–299.

Garzon, A., Bravo, I., Carrion-Jimenez, M.R., Rubio-Moraga, A., Albaladejo, J., 2015. Spectroscopic study on binding of gentisic acid to bovine serum albumin. Spectrochim. Acta 150, 26–33.

Hazra, S., Hossain, M., Kumar, G.S., 2013. Binding of isoquinoline alkaloids berberine, palmatine and coralyne to hemoglobin: structural and thermodynamic characterization studies. Mol. Biosyst. 9, 143–153.

He, W., Dou, H.J., Li, Z.G., Wang, X.G., Wang, L.J., Wang, R.Y., Chang, J.B., 2014. Investigation of the interaction between five alkaloids and human hemoglobin by fluorescence spectroscopy and molecular modeling. Spectrochim. Acta 123, 176–186.

Huerga-Gonzalez, V., Lage-Yusty, M.A., Lago-Crespo, M., Lopez-Hernandez, J., 2015. Comparison of methods for the study of ellagic acid in pomegranate juice beverages. Food Anal. Method 8, 2286–2293.

Ishtikhar, M., Ahmad, E., Siddiqui, Z., Ahmad, S., Khan, M.V., Zaman, M., Siddiqi, M.K., Nusrat, S., Chandel, T.I., Ajmal, M.R., Khan, R.H., 2018. Biophysical insight into the interaction mechanism of plant derived polyphenolic compound tannic acid with homologous mammalian serum albumins. Int. J. Biol. Macromol. 107, 2450–2464.

Khatun, S., Riyazuddeen, Yasmeen, S., Kumar, A., Subbarao, N., 2018. Calorimetric, spectroscopic and molecular modelling insight into the interaction of gallic acid with bovine serum albumin. J. Chem. Thermodyn. 122, 85–94.

Krishnan, S.P., Hiray, K.S., Vyas, S., 2018. A correlative multi-spectroscopy and docking study for the modeling of drug (Luteolin and Quercetin) binding to bovine serum slbumin-atool for the determination of binding characteristics to receptor proteins. Indian J. Pharm. Educ. 52, 492–504.

Larrosa, M., Garcia-Conesa, M.T., Espin, J.C., Tomas-Barberan, F.A., 2010. Ellagitannins, ellagic acid and vascular health. Mol. Asp. Med. 31, 513–539.

Li, X.R., Wang, S., 2015. Study on the interaction of (+)-catechin with human serum albumin using isothermal titration calorimetry and spectroscopic techniques. New J. Chem. 39, 386–395.

Ma, X.Y., Yu, C.Z., Wang, R., Ma, X.P., 2018. Mechanism of vegetable extracts on preventing the oxidation of chrome(III). J. Soc. Leather Technol. Chem. 102, 283–288.

Makarska-Bialokoz, M., Lipke, A., 2019. Study of the binding interactions between uric acid and bovine serum albumin using multiple spectroscopic techniques. J. Mol. Liq. 276, 595–604.

Nanda, R.K., Sarkar, N., Banerjee, R., 2007. Probing the interaction of ellagic acid with human serum albumin: a fluorescence spectroscopic study. J. Photochem. Photobiol.,

A 192, 152–158.
Papadopoulou, A., Green, R.J., Frazier, R.A., 2005. Interaction of flavonoids with bovine serum albumin: a fluorescence quenching study. J. Agric. Food Chem. 53, 158–163.
Patil, S., Sandberg, A., Heckert, E., Self, W., Seal, S., 2007. Protein adsorption and cellular uptake of cerium oxide nanoparticles as a function of zeta potential. Biomaterials 28, 4600–4607.
Promsong, A., Chuenchitra, T., Saipin, K., Tewtrakul, S., Panichayupakaranant, P., Satthakarn, S., Nittayananta, W., 2018. Ellagic acid inhibits HIV-1 infection in vitro: potential role as a novel microbicide. Oral Dis. 24, 249–252.
Quiming, N.S., Vergel, R.B., Nicolas, M.G., Villanueva, J.A., 2005. Interaction of bovine serum albumin and metallothionein. J. Health Sci. 51, 8–15.
Rudradip, P., Pijush, B., Srikanta, S., Maitree, B., 2017. An insight to the binding of ellagic acid with human serum albumin using spectroscopic and isothermal calorimetry studies. Biochem. Biophys. Rep. 10, 88–93.
Schmidt, S., Gonzalez, D., Derendorf, H., 2010. Significance of protein binding in pharmacokinetics and pharmacodynamics. J. Pharm. Sci. 99, 1107–1122.
Soong, Y.Y., Barlow, P.J., 2006. Quantification of gallic acid and ellagic acid from longan (Dimocarpus longan Lour.) seed and mango (Mangifera indica L.) kernel and their effects on antioxidant activity. Food Chem. 97, 524–530.
Szmagara, A., Krzyszczak, A., Sadok, I., Karczmarz, K., Staniszewska, M.M., Stefaniak, E.A., 2019. Determination of ellagic acid in rose matrix by spectrofluorimetry. J. Food Compos. Anal. 78, 91–100.
Tang, L., Jia, W., 2013. A comparison study on the binding of hesperetin and luteolin to bovine serum albumin by spectroscopy. Spectrochim. Acta A 103, 114–119.
Tasaki, M., Umemura, T., Maeda, M., Ishii, Y., Okamura, T., Inoue, T., Kuroiwa, Y., Hirose, M., Nishikawa, A., 2008. Safety assessment of ellagic acid, a food additive, in a subchronic toxicity study using F344 rats. Food Chem. Toxicol. 46, 1119–1124.
Trnkova, L., Bousova, I., Stankova, V., Drsata, J., 2011. Study on the interaction of catechins with human serum albumin using spectroscopic and electrophoretic techniques. J. Mol. Struct. 985, 243–250.
Wang, H.C., Jiang, X.H., Zhou, L.M., Cheng, Z.J., Yin, W.M., Duan, M., Liu, P.L., Jiang, X.M., 2013a. Interaction of NAEn-s-n gemini surfactants with bovine serum albumin: a structure-activity probe. J. Lumin. 134, 138–147.
Wang, L.F., Li, L.L., Ran, X.J., Long, M., Zhang, M.F., Tao, Y.C., Luo, X., Wang, Y., Ma, X.L., Halmurati, U., Mao, X.M., Ren, J., 2013b. Ellagic acid reduces adipogenesis through inhibition of differentiation-prevention of the induction of Rb phosphorylation in 3T3-L1 adipocytes. Evid. Based Complement Altern. Med. 2, 287534.
Wang, Y.Q., Zhang, H.M., Zhou, Q.H., 2009. Studies on the interaction of caffeine with bovine hemoglobin. Eur. J. Med. Chem. 44, 2100–2105.
Xu, T.C., Guo, X.J., Zhang, L., Pan, F., Lv, J.N., Zhang, Y.Y., Jin, H.J., 2012. Multiple spectroscopic studies on the interaction between olaquindox, a feed additive, and bovine serum albumin. Food Chem. Toxicol. 50, 2540–2546.
Yang, B.J., Hao, F., Li, J.R., Wei, K., Wang, W.Y., Liu, R.T., 2014. Characterization of the binding of chrysoidine, an illegal food additive to bovine serum albumin. Food Chem. Toxicol. 65, 227–232.
Yang, X., Tomas-Barberan, F.A., 2019. Tea is a significant dietary source of ellagitannins and ellagic acid. J. Agric. Food Chem. 67, 5394–5404.
Zhang, G.W., Wang, L., Pan, J.H., 2012. Probing the binding of the flavonoid diosmetin to human serum albumin by multispectroscopic techniques. J. Agric. Food Chem. 60, 2721–2729.
Zhang, H.M., Chen, T.T., Zhou, Q.H., Wang, Y.Q., 2009. Binding of caffeine, theophylline, and theobromine with human serum albumin: a spectroscopic study. J. Mol. Struct. 938, 221–228.
Zhong, C., Qiu, S., Li, J.L., Shen, J.L., Zu, Y.G., Shi, J.M., Sui, G.C., 2019. Ellagic acid synergistically potentiates inhibitory activities of chemotherapeutic agents to human hepatocellular carcinoma. Phytomedicine 59, 152921.
Zhou, B.H., Li, Q.L., Wang, J., Chen, P., Jiang, S., 2019. Ellagic acid attenuates streptozocin induced diabetic nephropathy via the regulation of oxidative stress and inflammatory signaling. Food Chem. Toxicol. 123, 16–27.